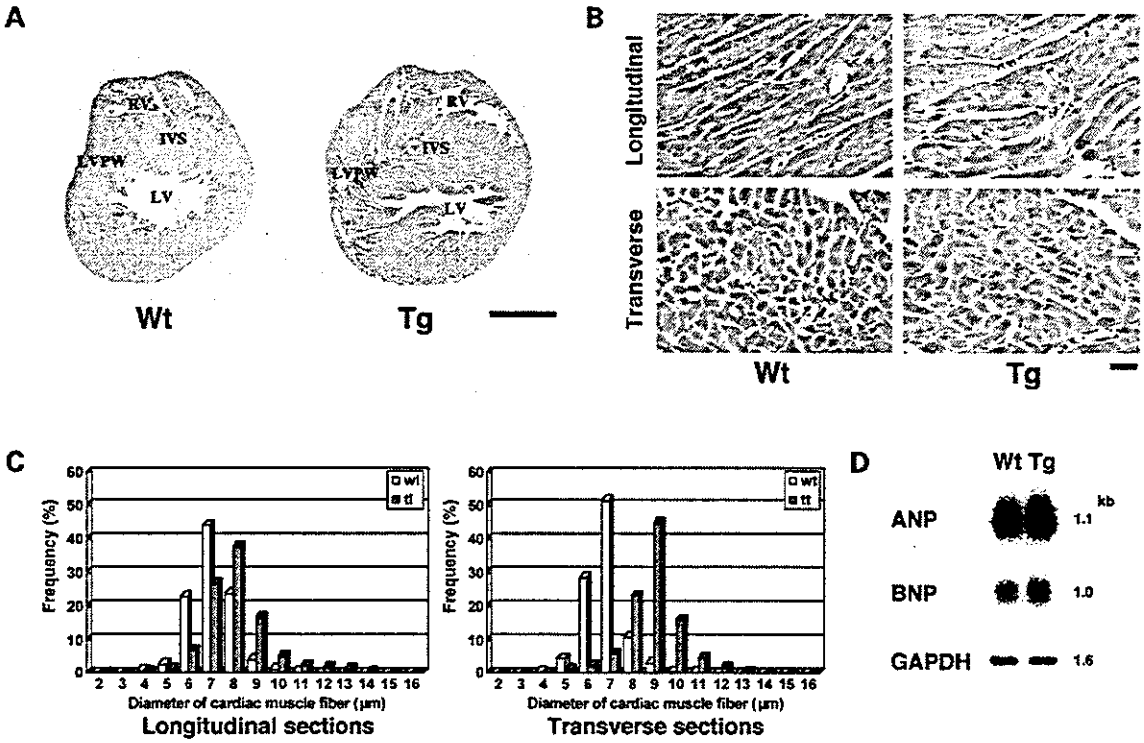

Figure 2. Histology of hearts from 6-week-old Wt and Tg mice. (A) Gross appearance of transverse lower ventricular sections from Wt and Tg mouse hearts. Note that apparent thickening of the interventricular septum and posterior wall of the left ventricle results in a tiny ventricular chamber in the Tg mouse heart (right). LV, left ventricle; IVS, interventricular septum; LVPW, left ventricular posterior wall; RV, right ventricle. Bar, 1 mm. (B) H&E staining of cardiac muscle sections from 6-week-old Wt or Tg mice. Note the myofiber hypertrophy in the Tg mouse hearts in both longitudinal (Upper panels) and transverse (lower panels) sections. Bar, 10 μm. (C) Histogram of cardiac myofiber diameter from 6-week-old Wt or Tg mice on longitudinal sections (left) and on transverse sections (right). The diameters of 1000 cardiac muscle fibers from five Tg mice and five Wt mice were measured. Note that the frequency distribution (%) of the cardiac muscle fiber diameter in the Tg mice compared with that in the Wt mice shows a skewed distribution to the right and marked size variability, thus indicating cardiac myocyte hypertrophy. The diameter of each cardiac muscle fiber was measured by the IBAS 2000 image analysis system (Zeiss). (D) Northern blot analysis of cardiac myocyte hypertrophic markers; ANP and BNP. Radiointensities of ANP and BNP transcripts in the Tg mouse hearts were up-regulated by 1.69- and 1.54-fold, respectively.

Table 1. Transthoracic echocardiographic analysis of hearts from 24-week-old Wt and Tg mice

Group	Interventricular septal thickness (mm)	Left ventricular posterior wall thickness (mm)	Left ventricular end diastolic diameter (mm)	Left ventricular end systolic diameter (mm)	Left ventricular fractional shortening (%)
Wt	0.83 ± 0.11	0.78 ± 0.08	3.94 ± 0.28	2.14 ± 0.23	45.60 ± 4.00
Tg	1.04 ± 0.12*	1.07 ± 0.11*	3.00 ± 0.30*	1.15 ± 0.18*	61.20 ± 4.70*

*$P < 0.01$. Wt ($n = 7$); Tg ($n = 7$).

NOS activity is increased in TgCAV3M1 mouse hearts

Expression of all NOS isoforms was similar when Wt and Tg mice cardiac muscles were compared by northern blot and immunoblot analyses (Fig. 4A and B). In addition, sub-sarcolemmal and vascular endothelial localization of eNOS was similar in Tg and Wt mouse hearts (Fig. 4C). NOS activity was quantified in crude extracts from freshly isolated hearts from six-week-old Wt and Tg mice ($n = 8$). Total NOS and eNOS activities in the Tg mouse hearts were significantly higher ($P < 0.05$) than those in the Wt mouse hearts: total NOS activity (pmol/mg protein/min)—Tg mouse, 5.10 ± 0.32, Wt mouse, 3.38 ± 0.32; eNOS activity (pmol/mg protein/min)—Tg mouse, 4.03 ± 0.32, Wt mouse, 2.31 ± 0.24. No significant differences were observed in either nNOS activity (pmol/mg protein/min)—Tg mouse, 0.77 ± 0.07, Wt mouse, 0.75 ± 0.06—or iNOS activity (pmol/mg protein/min)—Tg mouse, 0.30 ± 0.02, Wt mouse, 0.31 ± 0.03 (Fig. 4D).

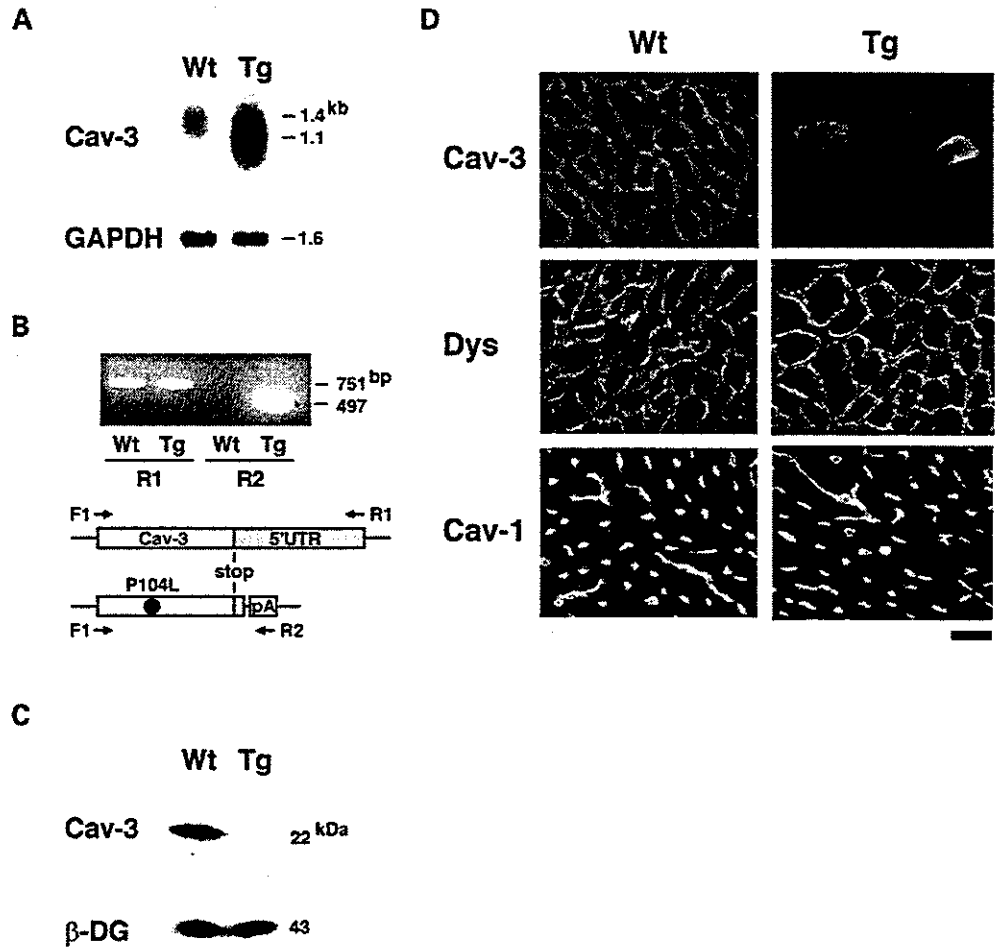

Figure 3. (A) Northern blot analysis of caveolin-3 in cardiac muscle from 6-week-old Wt and Tg mice. The smaller-sized (~1.1 kb) mutant caveolin-3 mRNA was expressed excessively in the Tg mice compared with the Wt mice. (B) RT–PCR analysis of endogeneous or mutant caveolin-3 in cardiac muscle from 6-week-old Wt and Tg mice. The endogenous caveolin-3 was detectable in Tg mice as well as Wt mice using primers of F1/R1 (upper panel, left). The mutant caveolin-3 mRNA was detectable only in Tg mice using primers of F1/R2 (upper panel, right). R1 corresponds to the 5′-untranslated region (5′-UTR) of the caveolin-3 transcript, whereas R2 corresponds to the SV40 polyadenylation site (pA) of the transgene transcript (lower panel). (C) Immunoblot analysis of caveolin-3 in total protein extracts from 6-week-old Wt and Tg mouse cardiac muscles. Caveolin-3 expression was markedly reduced in the Tg mice. In contrast, β-DG expression was similar in the Wt and Tg mice. (D) Immunohistochemical analysis of cardiac muscle from 6-week-old Wt and Tg mice. Lower ventricular cryosections from the Wt and Tg mice were stained with antibodies against caveolin-3 (Cav-3), dystrophin (Dys) and caveolin-1 (Cav-1). Caveolin-3 localized to the sarcolemma in the Wt mice, but the Tg mice generally lacked caveolin-3 except for a few fibers that showed weak cytoplasmic localization of caveolin-3. The expression of dystrophin and caveolin-1 was similar in the Wt and Tg mice. Bar, 10 μm.

DISCUSSION

Caveolin-3 is a strong physiological inhibitor of NOS and expressed specifically in cardiac and skeletal myocytes (5–8). The present study demonstrated the occurrence of hypertrophic cardiomyopathy with enhanced contractility in association with increased eNOS activity in caveolin-3-deficient transgenic mice without changes in NOS expression. Therefore, loss of NOS inhibition secondary to deficient caveolin-3 may contribute to the pathogenesis of hypertrophic cardiomyopathy.

NOS activity may modulate cardiac contractility and architecture (15–18). eNOS is localized in caveolae (5,8) and plays a role in inhibition of β-adrenergic-induced contractility (19,20). NO generated by eNOS may also interact with the SR ryanodine receptor (21). In contrast, nNOS, located in the SR (15,22), increases SR Ca^{2+} release and enhances cardiac contractility (15,23). eNOS knockout mice show enhanced contractility (15), while overexpression of eNOS results in reduced cardiac size and contractility (24). Unexpectedly, our Tg mouse hearts with moderately increased eNOS activity showed enhanced

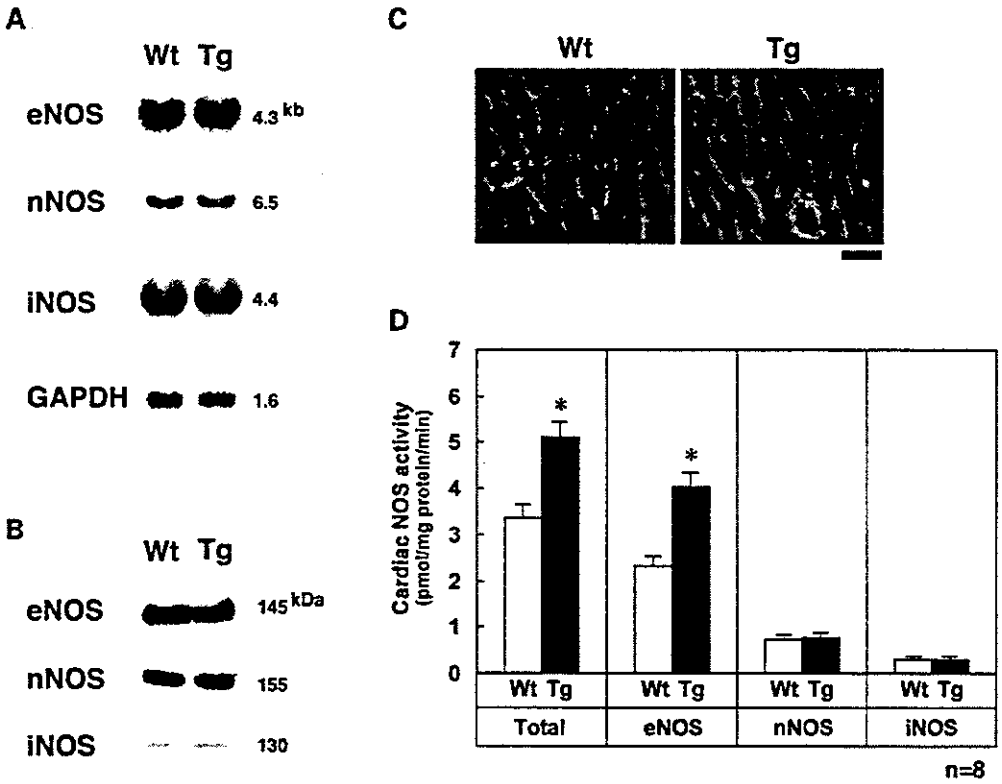

Figure 4. Northern blot analysis (**A**) and immunoblot analysis (**B**) of NOS isoforms in cardiac muscle from 6-week-old Wt and Tg mice. Note the comparable expression of all NOS isoforms in the Wt and Tg mice. (**C**) Immunohistochemical analysis of eNOS in cardiac muscle from 6-week-old Wt and Tg mice. The expression pattern of eNOS was similar in the Wt and Tg mice. Bar, 10 μm. (**D**) NOS activities in crude extracts from cardiac muscle from 6-week-old Wt and Tg mice. Note that significant increases in total NOS and eNOS activity were observed in the Tg mice, compared to the Wt mice ($n = 8$). In contrast no significant difference was observed in either nNOS or iNOS activity between the Tg and Wt mice. Data are expressed as mean ± SD. *Statistical significance was determined using Welch's t-test ($P < 0.05$).

contractility and hypertrophic cardiomyopathy. It is noteworthy that exogenous NO, derived from pharmacological NO donors, produces a biphasic contractile response in cardiac tissue with augmentation at low NO levels and depression at high NO levels (25–27). Based on these exogenous NO donor experiments, we postulate that a moderate activation of eNOS activity, as seen in the mutant caveolin-3 Tg mouse hearts enhances contractility and leads to hypertrophic cardiomyopathy, whereas an extremely high activation of eNOS activity, as seen in mouse hearts in which eNOS is overexpressed, reduces contractility and cardiac size.

Woodman *et al.* (28) reported that caveolin-3 null mice showed cardiomyopathy and suppressed contractility, possibly secondary to alterations in the p42/44 MAPK pathway, but they did not characterize changes in NOS isoform profiles. Based on previous studies and the present data, we would predict greater NOS activity in caveolin-3 null mouse hearts than in the hearts of mutant caveolin-3 transgenic mice. This higher NOS activity in caveolin-3 null mouse hearts may result in suppression of cardiac contractility.

To date hypertrophic cardiomyopathy has not been reported in LGMD1C patients. However, in only one German pedigree of autosomal dominant rippling muscle disease (AD-RMD) (29), which was proven to carry a caveolin-3 missense mutation (A45V) (10), two patients died suddenly of possible cardiac arrhythmia. An autopsy study of one patient in this pedigree disclosed non-obstructive cardiomyopathy, which was poorly described (29). Cardiac involvement, cardiomyopathy and/or arrhythmia may be a rare but possible feature of CAV-3 missense mutations. Further extensive clinical examination of cardiac function in LGMD1C patients is necessary to test this possibility. Furthermore, it is plausible that the higher copy number of the mutant caveolin-3 gene in TgCAV3M1 mice promotes a disease process leading to HCM.

In conclusion, we propose that moderate eNOS activation caused by loss of caveolin-3 may be involved in a caveolin-3-mediated hypertrophic signal pathway of cardiac myocytes.

MATERIALS AND METHODS

RT–PCR

cDNA templates were reverse-transcribed from 1 μg of total RNA from mouse cardiac muscle, primed with an oligo$(dT)_{12-18}$

primer and then subjected to PCR. For amplification of the endogenous caveolin-3 gene, we used F1 (5′-CCCAGCCTCACAAT GATGACCGAAG-3′) and R1 (5′-CATGTGAACGCAAAGCC TTGC-3′). For amplification of the transgene, we used F1 and R2 (5′-GCATTCTAGTTGTGGTTT-3′). As illustrated in Figure 3B, R1 and R2 correspond to the 5′-untranslated region of caveolin-3 cDNA and the SV40 polyadenylation site, respectively, as described previously (11).

Northern blot analysis

RT–PCR product of endogenous caveolin-3 was subcloned into TA vector pCR2.1 (Invitrogen) and then digested by *Eco*RI. The digested insert was extracted from agarose gel using Concert Kit (GibcoBRL). This cDNA was then labeled as a probe with [α-^{32}P]dCTP using MegaPrime DNA labeling system (Amersham Pharmacia Biotech). Ten micrograms of total RNA from 6-week-old Wt and Tg cardiac muscle were separated on 0.7% agarose gels containing 7% formaldehyde and blotted onto Hybond-N+ (Amersham Pharmacia Biotech). Hybridization was performed at 42°C for 12–24 h and autoradiography was performed on a Fuji imaging plate (Fuji Film). Signal intensity of transcripts was measured by BAS2000 Image Analyzer (Fuji Film). Using the same method, we hybridized northern blots with RT–PCR generated and labeled fragments of ANP cDNA, BNP cDNA, eNOS cDNA, nNOS cDNA, iNOS cDNA and internal control GAPDH cDNA.

Immunoblot analysis

Six-week-old Wt or Tg mouse cardiac muscle was homogenized in 10 vols (w/v) of a buffer containing 50 mM Tris–HCl (pH 7.4), 100 mM NaCl, 1 mM ethylenediaminetetraacetic acid (EDTA), 5 mM β-mercaptoethanol, 0.1 mM phenylmethylsulphonyl fluoride (PMSF) and 1 mM benzamidine. These crude extracts were denatured and size fractionated by SDS–PAGE (3–12%) and then transferred to a polyvinylidine difluoride (PVDF) membrane. The membrane was blocked using 5% milk in phosphate-buffered saline (PBS) and incubated with rabbit polyclonal antibody against caveolin-3 (Transduction Laboratories, C38330), raised against synthetic peptide corresponding to the amino terminus of caveolin-3 of rat and mouse origin, a monoclonal antibody against β-dystoglycan (Novo Castra), a rabbit polyclonal antibody against eNOS (Santa Cruz Biotechnology), a rabbit polyclonal antibody against nNOS (Santa Cruz Biotechnology) and a rabbit polyclonal antibody against iNOS (Transduction Laboratories) overnight at room temperature. After washing with 5% milk in PBS, the blots were incubated with horseradish peroxidase-conjugated anti-rabbit or anti-mouse IgG antibody (Amersham Pharmacia Biotech). Immunoreactive bands were visualized with ECL (Amersham Pharmacia Biotech).

Immunohistochemical analysis

Unfixed cardiac muscle samples were snap frozen in liquid nitrogen-cooled isopentane, sectioned on a cryostat (10 μm), and melted directly onto glass slides. Sections were then post-fixed in 4% freshly depolymerized paraformaldehyde in PBS for 15–30 min at 4°C. After blocking with 3% BSA in PBS, sections were immunostained with a goat polyclonal antibody against caveolin-3 (Santa Cruz Biotechnology, *sc-7665*), recognizing the epitope mapped at the amino terminus of caveolin-3 of mouse origin, a rabbit polyclonal antibody against caveolin-1 (Santa Cruz Biotechnology), a goat polyclonal antibody against dystrophin (Santa Cruz Biotechnology), and a rabbit polyclonal antibody against eNOS (Santa Cruz Biotechnology) for 1 h at room temperature. After extensive washing with PBS, sections were incubated with FITC-conjugated or Cy3-conjugated secondary antibody. Rabbit and goat polyclonal antibodies against caveolin-3 used in immunoblot and immunohistochemical analyses can recognize both mutant and wild type forms of caveolin-3.

Transthoracic echocardiogram

Transthoracic echocardiography was performed on 24-week-old Tg mice and Wt littermates ($n = 7$) under light anesthesia using intraperitoneal pentobarbital as described previously (30).

NOS assay

Total NOS activity was measured by monitoring the conversion of L-[^{3}H]arginine to L-[^{3}H]citrulline, as previously described (18,31–33). Briefly, freshly prepared cardiac muscle from 6-week-old Tg mice and Wt littermates ($n = 8$) was homogenized in 10 vols (w/v) of a buffer containing 50 mM Tris–HCl (pH 7.4), 100 mM NaCl, 0.5 mM EDTA, 0.5 mM EGTA, 1 mM DTT, 0.1 mM PMSF, and 1 μM leupeptin. Aliquots from crude homogenates were quickly assayed in 100 μl reactions containing 100 000 cpm (40 Ci/mmol) of L-[^{3}H]arginine, 1 mM NADPH, 50 mM Tris–HCl (pH 7.4), 100 mM NaCl, 1.2 mM $CaCl_2$, 10 μg/ml calmodulin, 1 mM DTT and 10 μM each of tetrahydrobiopterin, FAD and FMN. After an incubation of 10 min at 37°C, assays were terminated with 900 μl of ice cold H_2O. After brief sonication, samples were applied to 2 ml of Dowex AG 50W-X8 (Na^+ form) column. L-[^{3}H]citrulline was quantified using 1 ml flow-through by liquid scintillation spectroscopy. The combined activity of eNOS plus iNOS was also measured in the same reaction buffer containing specific inhibitor of nNOS (0.1 μM N^{ω}-propyl-L-arginine) (TOCRIS) (34,35). iNOS activity was also measured in the presence of 1.5 mM EDTA and 1.5 mM EGTA, which replaced Ca^{2+} ion in the reaction buffer. The above three assays were performed simultaneously. Then, nNOS activity was calculated by subtraction of the combined activity of eNOS and iNOS from total NOS activity. eNOS activity was calculated by subtraction of iNOS activity from the combined activity of eNOS and iNOS. Data are expressed as mean ± SD. Statistical significance was determined using Welch's *t*-test ($P < 0.05$).

ACKNOWLEDGEMENTS

We thank Drs Tsutomu Ogura, Yukiko Kurashima (Investigative Treatment Division, National Cancer Center Research Institute East) and Hiroshi Shima (Division of Biochemical Oncology and Immunology, Institute for Genetic Medicine, Hokkaido University) for their appropriate advice about the NOS assay method. We also thank Kenzo Uehira (Electron Microscopy Center, Kawasaki Medical School) and Megumu

Kita (Laboratory Animal Center, Kawasaki Medical School) for their technical assistance. This work was supported by Research Grant (14B-4) for Nervous and Mental Disorders from the Ministry of Health, Labour and Welfare, Research Grant (15130301) for Research on Psychiatric and Neurological Diseases and Mental Health from the Ministry of Health, Labour and Welfare, Research Grant (14370212) from the Ministry of Education, Culture, Sports, Science and Technology, and Research Project Grants (no. 13-105, 14-117, 14-505, 14604 and 14-208) from Kawasaki Medical School.

REFERENCES

1. Razani, B., Schlegel, A. and Lisanti, M.P. (2000) Caveolin proteins in signaling, oncogenic transformation and muscular dystrophy. *J. Cell Sci.*, **113**, 2103–2109.
2. Monier, S., Parton, R.G., Vogel, F., Behlke, J., Henske, A. and Kurzchalia, T.V. (1995) VIP21-caveolin, a membrane protein constituent of the caveolar coat, oligomerizes *in vivo* and *in vitro*. *Mol. Biol. Cell*, **6**, 911–927.
3. Couet, J., Li, S., Okamoto, T., Ikezu, T. and Lisanti, M.P. (1997) Identification of peptide and protein ligands for the caveolin-scaffolding domain. Implications for the interaction of caveolin with caveolae-associated proteins. *J. Biol. Chem.*, **272**, 6525–6533.
4. Galbiati, F., Razani, B. and Lisanti, M.P. (2001) Emerging themes in lipid rafts and caveolae. *Cell*, **106**, 403–411.
5. Feron, O., Belhassen, L., Kobzik, L., Smith, T.W., Kelly, R.A. and Michel, T. (1996) Endothelial nitric oxide synthase targeting to caveolae. Specific interactions with caveolin isoforms in cardiac myocytes and endothelial cells. *J. Biol. Chem.*, **271**, 22810–22814.
6. Kobzik, L., Reid, M.B., Bredt, D.S. and Stamler, J.S. (1994) Nitric oxide in skeletal muscle. *Nature*, **372**, 546–548.
7. Venema, V.J., Ju, H., Zou, R. and Venema, R.C. (1997) Interaction of neuronal nitric-oxide synthase with caveolin-3 in skeletal muscle. Identification of a novel caveolin scaffolding/inhibitory domain. *J. Biol. Chem.*, **272**, 28187–28190.
8. Garcia-Cardena, G., Martasek, P., Masters, B.S., Skidd, P.M., Couet, J., Li, S., Lisanti, M.P. and Sessa, W.C. (1997) Dissecting the interaction between nitric oxide synthase (NOS) and caveolin. Functional significance of the NOS caveolin binding domain *in vivo*. *J. Biol. Chem.*, **272**, 25437–25440.
9. Minetti, C., Sotgia, F., Bruno, C., Scartezzini, P., Broda, P., Bado, M., Masetti, E., Mazzocco, M., Egeo, A., Donati, M.A. *et al.* (1998) Mutations in the caveolin-3 gene cause autosomal dominant limb-girdle muscular dystrophy. *Nat. Genet.*, **18**, 365–368.
10. Betz, R.C., Schoser, B.G., Kasper, D., Ricker, K., Ramirez, A., Stein, V., Torbergsen, T., Lee, Y.A., Nothen, M.M., Wienker, T.F. *et al.* (2001) Mutations in CAV3 cause mechanical hyperirritability of skeletal muscle in rippling muscle disease. *Nat. Genet.*, **28**, 218–219.
11. Sunada, Y., Ohi, H., Hase, A., Ohi, H., Hosono, T., Arata, S., Higuchi, S., Matsumura, K. and Shimizu, T. (2001) Transgenic mice expressing mutant caveolin-3 show severe myopathy associated with increased nNOS activity. *Hum. Mol. Genet.*, **10**, 173–178.
12. Fujita, T., Toya, Y., Iwatsubo, K., Onda, T., Kimura, K., Umemura, S. and Ishikawa, Y. (2001) Accumulation of molecules involved in alpha1-adrenergic signal within caveolae: caveolin expression and the development of cardiac hypertrophy. *Cardiovasc. Res.*, **51**, 709–716.
13. Winlaw, D.S., Smythe, G.A., Keogh, A.M., Schyvens, C.G., Spratt, P.M. and Macdonald, P.S. (1994) Increased nitric oxide production in heart failure. *Lancet*, **344**, 373–374.
14. Stein, B., Eschenhagen, T., Rudiger, J., Scholz, H., Forstermann, U. and Gath, I. (1998) Increased expression of constitutive nitric oxide synthase III, but not inducible nitric oxide synthase II, in human heart failure. *J. Am. Coll. Cardiol.*, **32**, 1179–1186.
15. Barouch, L.A., Harrison, R.W., Skaf, M.W., Rosas, G.O., Cappola, T.P., Kobeissi, Z.A., Hobai, I.A., Lemmon, C.A., Burnett, A.L., O'Rourke, B. *et al.* (2002) Nitric oxide regulates the heart by spatial confinement of nitric oxide synthase isoforms. *Nature*, **416**, 337–341.
16. Balligand, J.L., Kelly, R.A., Marsden, P.A., Smith, T.W. and Michel, T. (1993) Control of cardiac muscle cell function by an endogenous nitric oxide signaling system. *Proc. Natl Acad. Sci. USA*, **90**, 347–351.
17. Klabunde, R.E., Kimber, N.D., Kuk, J.E., Helgren, M.C. and Forstermann, U. (1992) N^G-methyl-L-arginine decreases contractility, cGMP and cAMP in isoproterenol-stimulated rat hearts *in vitro*. *Eur. J. Pharmac.*, **223**, 1–7.
18. Balligand, J.L., Kobzik, L., Han, X., Kaye, D.M., Belhassen, L., O'Hara, D.S., Kelly, R.A., Smith, T.W. and Michel, T. (1995) Nitric oxide-dependent parasympathetic signaling is due to activation of constitutive endothelial (type III) nitric oxide synthase in cardiac myocytes. *J. Biol. Chem.*, **270**, 14582–14586.
19. Hare, J.M., Lofthouse, R.A., Juang, G.J., Colman, L., Ricker, K.M., Kim, B., Senzaki, H., Cao, S., Tunin, R.S. and Kass, D.A. (2000) Contribution of caveolin protein abundance to augmented nitric oxide signaling in conscious dogs with pacing-induced heart failure. *Circul. Res.*, **86**, 1085–1092.
20. Hare, J.M., Givertz, M.M., Creager, M.A. and Colucci, W.S. (1998) Increased sensitivity to nitric oxide synthase inhibition in patients with heart failure: potentiation of β-adrenergic inotropic responsiveness. *Circulation*, **97**, 161–166.
21. Vila-Petroff, M.G., Kim, S.H., Pepe, S., Dessy, C., Marban, E., Balligand, J.L. and Sollott, S.J. (2001) Endogenous nitric oxide mechanisms mediate the stretch dependence of Ca^{2+} release in cardiomyocytes. *Nat. Cell. Biol.*, **3**, 867–873.
22. Xu, K.Y., Huso, D.L., Dawson, T.M., Bredt, D.S. and Becker, L.C. (1999) Nitric oxide synthase in cardiac sarcoplasmic reticulum. *Proc. Natl Acad. Sci. USA*, **96**, 657–662.
23. Xu, L., Eu, J.P., Meissner, G. and Stamler, J.S. (1998) Activation of the cardiac calcium release channel (ryanodine receptor) by poly-*S*-nitrosylation. *Science*, **279**, 234–237.
24. Brunner, F., Andrew, P., Wolkart, G., Zechner, R. and Mayer, B. (2001) Myocardial contractile function and heart rate in mice with myocyte-specific overexpression of endothelial nitric oxide synthase. *Circulation*, **104**, 3097–3102.
25. Mery, P.F., Pavoine, C., Belhassen, L., Pecker, F. and Fischmeister, R. (1993) Nitric oxide regulates cardiac Ca^{2+} current. Involvement of cGMP-inhibited and cGMP-stimulated phosphodiesterases through guanylyl cyclase activation. *J. Biol. Chem.*, **268**, 26286–26295.
26. Vila-Petroff, M.G., Younes, A., Egan, J., Lakatta, E.G. and Sollott, S.J. (1999) Activation of distinct cAMP-dependent and cGMP-dependent pathways by nitric oxide in cardiac myocytes. *Circul. Res.*, **84**, 1020–1031.
27. Shah, A.M., Spurgeon, H.A., Sollott, S.J., Talo, A. and Lakatta, E.G. (1994) 8-bromo-cGMP reduces the myofilament response to Ca^{2+} in intact cardiac myocytes. *Circul. Res.*, **74**, 970–978.
28. Woodman, S.E., Park, D.S., Cohen, A.W., Cheung, M.W., Chandra, M., Shirani, J., Tang, B., Jelicks, L.A., Kitsis, R.N., Christ, G.J. *et al.* (2002) Caveolin-3 knock-out mice develop a progressive cardiomyopathy and show hyperactivation of the p42/44 MAPK cascade. *J. Biol. Chem.*, **277**, 38988–38997.
29. Ricker, K., Moxley, R.T. and Rohkamm, R. (1989) Rippling muscle disease. *Arch. Neurol.*, **46**, 405–408.
30. Toko, H., Oka, T., Zou, Y., Sakamoto, M., Mizukami, M., Sano, M., Yamamoto, R., Sugaya, T. and Komuro, I. (2002) Angiotensin II type 1a receptor mediates doxorubicin-induced cardiomyopathy. *Hypertens. Res.*, **25**, 597–603.
31. Bredt, D.S. and Snyder, S.H. (1990) Isolation of nitric oxide synthase, a calmodulin-requiring enzyme. *Proc. Natl Acad. Sci. USA*, **87**, 682–685.
32. Shulz, R., Nava, E. and Moncada, S. (1992) Induction and potential biological relevance of a Ca^{2+}-independent nitric oxide synthase in the myocardium. *Br. J. Pharmac.*, **105**, 575–580.
33. Bia, B.L., Cassidy, P.J., Young, M.E., Rafael, J.A., Leighton, B., Davies, K.E., Radda, G.K. and Clark, K. (1999) Decreased myocardial nNOS, increased iNOS and abnormal ECGs in mouse models of Duchenne muscular dystrophy. *J. Mol. Cell. Cardiol.*, **31**, 1857–1862.
34. Zhang, H.Q., Fast, W., Marletta, M.A., Martasek, P. and Silverman, R.B. (1997) Potent and selective inhibition of neuronal nitric oxide synthase by N^{ω}-propyl-L-arginine. *J. Med. Chem.*, **40**, 3869–3870.
35. Kakoki, M., Zou, A.-P. and Mattson., D.L. (2001) The influence of nitric oxide synthase 1 on blood flow and interstitial nitric oxide in the kidney. *Am. J. Physiol. Regul. Integr. Comp. Physiol.*, **281**, R91–R97.

The FASEB Journal express article 10.1096/fj.03-0637fje. Published online March 4, 2004.

Cytokine therapy prevents left ventricular remodeling and dysfunction after myocardial infarction through neovascularization

Masashi Ohtsuka,* Hiroyuki Takano,* Yunzeng Zou,* Haruhiro Toko,* Hiroshi Akazawa,* Yingjie Qin,* Masashi Suzuki,† Hiroshi Hasegawa,* Haruaki Nakaya,† and Issei Komuro*

*Department of Cardiovascular Science and Medicine and †Department of Pharmacology, Chiba University Graduate School of Medicine, 1-8-1 Inohana, Chuo-ku, Chiba 260-8670, Japan

Corresponding author: Issei Komuro, Department of Cardiovascular Science and Medicine, Chiba University Graduate School of Medicine. 1-8-1 Inohana, Chuo-ku, Chiba 260-8670, Japan. E-mail: komuro-tky@umin.ac.jp

ABSTRACT

Pretreatment with a combination of granulocyte colony-stimulating factor (G-CSF) and stem cell factor (SCF) has been reported to attenuate left ventricular (LV) remodeling after acute myocardial infarction (MI). We here examined whether the cytokine treatment started after MI has also beneficial effects. Anterior MI was created in the recipient mice whose bone marrow had been replaced with that of transgenic mice expressing enhanced green fluorescent protein (GFP). We categorized mice into five groups according to the following treatment: 1) saline; 2) administration of G-CSF and SCF from 5 days before MI through 3 days after; 3) administration of G-CSF and SCF for 5 days after MI; 4) administration of G-CSF alone for 5 days after MI; 5) administration of SCF alone for 5 days after MI. All the three treatment groups with G-CSF showed less LV remodeling and improved cardiac function and survival rate after MI. The number of capillaries, which express GFP, was increased and the number of apoptotic cells was decreased in the border area of all the treatment groups with G-CSF. Even if the cytokine treatment is started after MI, it could prevent LV remodeling and dysfunction after MI—at least in part—through an increase in neovascularization and a decrease in apoptosis in the border area.

Key words: apoptosis • bone marrow • G-CSF

It is important to prevent left ventricular (LV) remodeling after acute myocardial infarction (MI) because it causes heart failure and poor prognosis (1). After MI, many cardiomyocytes undergo cell death by the mechanisms of necrosis and apoptosis in the infarcted area, which is then replaced by fibrotic tissue. The infarcted area is gradually extended by the subsequent death of cardiomyocytes in the border area and expanded by abnormal wall tension (2). Myocardial ischemia plays a critical role in the cardiomyocyte death in the border area after MI and thus greatly affects LV remodeling (2). Recently, Orlic et al. have reported that a subset of bone marrow stem cells (BMSCs) differentiate into cardiomyocytes when injected into peri-infarcted area, which results in regeneration of the infarcted heart (3). They have also reported that a pretreatment with granulocyte colony-stimulating factor (G-CSF) and stem cell factor (SCF), which strongly induce mobilization of BMSCs from bone marrow (BM), attenuates LV remodeling after MI (4–6). Although these results suggest that the cytokine treatment is beneficial

to prevent LV remodeling, the cytokine treatment was started before MI and thus this protocol cannot be applied to humans. Furthermore, the molecular mechanism of how the cytokine treatment repairs the infarcted heart is not fully understood.

In the present study, we examined three points: 1) whether the cytokine treatment started after MI is as effective as the pretreatment; 2) whether the combination treatment with G-CSF and SCF is more effective than the single treatment with G-CSF alone or SCF alone; and 3) how G-CSF prevents LV remodeling and dysfunction after MI. We used mice that were replaced by BM cells of enhanced green fluorescent protein (GFP)-expressing mice to elucidate the role of BM cells in the reduction of infarct size.

MATERIALS AND METHODS

Murine MI model

C57BL/6 male mice at 12-weeks-old were used in this study. All protocols were approved by the Institutional Animal Care and Use Committee of Chiba University. Mice were anesthetized with pentobarbital and artificially ventilated with a respirator, and MI was produced by permanent ligation of the left coronary artery with a 10-0 nylon surgical suture under a dissecting microscope as previously described (7). Sham operation was performed by cutting pericardium.

Cytokine treatments

Mice were divided into the following five groups: 1) administration of vehicle (control, n=22); 2) administration of G-CSF (100 μg/kg/day, Kyowa Hakko Kogyo Co., LTD. Tokyo, Japan) and SCF (200 μg/kg/day, Kirin Brewery Co., LTD. Tokyo, Japan) from 5 days before MI through 3 days after (Pre-GS, n=16); 3) administration of G-CSF (100 μg/kg/day) and SCF (200 μg/kg/day) for 5 days after MI (Post-GS, n=20); 4) administration of G-CSF (100 μg/kg/day) alone for 5 days after MI (Post-G, n=20); 5) administration of SCF (200 μg/kg/day) alone for 5 days after MI (Post-S, n=21). We gave first injection of vehicle, G-CSF, or SCF at 2 h after MI subcutaneously (Fig. 1*A*). In addition, we added a sham-operated group (n=5) to clarify whether cytokine treatments act completely or partly on MI heart.

Physiological analysis

For physiological analysis, we examined hemodynamic parameters of the survived mice (Sham, n=5; Control, n=5; Pre-GS, n=10; Post-GS, n=16; Post-G, n=14; Post-S, n=9) at 2 weeks after MI by cardiac catheterization. Mice were anesthetized by intraperitoneal injection of a mixture of 100 mg/kg ketamine (Sigma Chemical Co., St. Louis, MO) and 5 mg/kg xylazine (Sigma). The right carotid artery was cannulated by Millar Mikro-Tip transducer (model SPR-612, Millar Instruments, Houston, TX) as described previously (8). Pressure signals were recorded by using MacLab 3.6/s data acquisition system (AD Instruments, Milford, MA) with sampling rate 2000 Hz. LV systolic pressure (LVP), LV end-diastolic pressure (LVEDP), and positive and negative first derivatives for maximal rates of LV pressure development (dP/dt and –dP/dt) were measured.

Histological analysis

We excised hearts (Sham, n=5; Control, n=5; Pre-GS, n=10; Post-GS, n=16; Post-G, n=14; Post-S, n=9) for histological analysis after catheterization. LV was fixed with 10% formalin overnight and dehydrated methanol and was embedded in paraffin. Serial sections at 4 μm were stained with hematoxylin-eosin and Azan-Mallory. The scar area was evaluated by tracing the blue area in Azan-Mallory staining. We evaluated LV remodeling as described previously (9).

Capillary density, inflammatory cells, and apoptotic cell death

We analyzed inflammatory cells, capillary density, and apoptotic cells by another series of experiment (Control, n=5; Pre-GS, n=5; Post-GS, n=5; Post-G, n=5). The capillaries in the border area of MI hearts were identified by staining endothelial cells with antibody against platelet/endothelial cell adhesion molecule-1(PECAM-1; Santa Cruz Biotechnology, Santa Cruz, CA; 10). The number of capillaries per square millimeter was counted in the border area of MI hearts at 4 days after MI. Twenty fields of 200 μm × 200 μm for the border area were analyzed for each mouse at a magnification of × 400/high-power field (HPF). The inflammatory cells in the border area of MI hearts were identified with anti-Ly6G antibody (granulocytes), anti-Mac3antibody (macrophages), and anti-CD3 antibody (T-lymphocytes; BD PharMingen, San Diego, CA) at 4 day after MI. Furthermore, we performed an additional experiment to analyze apoptotic cells by TUNEL method at Days 1, 4, and 7 after MI (Control, n=15; Post-G, n=15). TUNEL assay was performed with an apoptosis detection kit (Takara Syuzo, Kyoto, Japan) as described previously (11). Furthermore, we examined double-immunohistochemical analysis with anti-von Willebrand factor antibody (DAKO, A/S, Denmark) to identify apoptotic endothelial cells.

Bone marrow transplantation

BM cells of GFP transgenic mice (12) were transplanted into C57BL/6 male mice as described previously (13). Flow cytometry analysis revealed that the BM chimerism was more than 70%. BM cells were identified by immunostaining with anti-GFP antibody (Medical and Biological Laboratories. CO., Nagoya, Japan) as described previously (14).

Statistics

All data are presented as mean ± SD. Multiple group comparison was performed by one-way ANOVA followed by the Bonferroni procedure for comparison of means. Survival rates of mice were analyzed by Kaplan-Meier method. Probability values less than 0.05 were considered to be statistically significant.

RESULTS

Mortality

The survival rates of mice at 14 days after MI were significantly higher in the three cytokine treatment groups with G-CSF (pre-GS, 63%; post-GS, 80%; and post-G, 70%) than in the control group (23%, P<0.05) and the post-S group (43%, P<0.05) in Kaplan-Meier method (Fig. 1*B*). There was no significant difference in the survival rates between pre- and post-treatment with

cytokines and between the combination treatment with G-CSF and SCF, and the treatment with G-CSF alone.

Physiological analysis

In the present study, we examined cardiac function by echocardiogram a few days before grouping. The mice with normal cardiac function were used in this study. Therefore, the degree of baseline LV function in mouse was equal among the groups before entry for the study. At 2 weeks after MI, there was no significant difference in the heart rate among all the groups (data not shown). LVP was higher in the three cytokine treatment groups with G-CSF than in the control group and the post-S group (Table 1). LVEDP was elevated in the control group and the post-S group but not the three treatment groups with G-CSF (Table 1). Furthermore, dP/dt and –dP/dt were larger in the three treatment groups with G-CSF than in control group and post-S group (Table 1). There was no significant difference in these parameters among the three cytokine treatment groups with G-CSF. These results suggest that all the three cytokine treatments with G-CSF improve systolic and diastolic functions of LV after MI.

Histological analysis

After MI, LV free wall was very thin and LV cavity was markedly expanded in control group and post-S group but LV wall thickness and LV cavity were preserved normal in the three treatment groups with G-CSF (Fig. 2*A*). Although the percentage of fibrotic area to the whole LV area was similar among cytokine treatment groups and the control group (control, 38.9 ± 9.7%; pre-GS, 35.2 ± 3.4%; post-GS, 33.1 ± 11.0%; post-G, 32.0. ± 5.4%; post-S, 32.8 ± 4.2%; Fig. 2*B*), the wall thickness was greater in the three cytokine treatment groups with G-CSF (sham, 1.14 ± 0.06 mm; pre-GS, 0.52 ± 0.14 mm; post-GS, 0.57 ± 0.20 mm; post-G, 0.53. ± 0.16 mm) than in control group (0.23 ± 0.07 mm) and post-S group (0.31 ± 0.08 mm; Fig. 2*C*). There was no significant difference in the wall thickness among all the three treatment groups with G-CSF.

Infiltration of white blood cells

G-CSF has been reported to increase the number of peripheral granulocytes (15). In this study, the number of granulocytes at 4 days after MI was higher in the three treatment groups (pre-GS, 12886 ± 773/mm^3; post-GS, 13912 ± 1447/mm^3; and post-G, 14318 ± 2736/mm^3) than in the control group (3056 ± 959/mm^3, P<0.05), but there was no histological evidence suggesting immunoreactions in all organs examined in our animal model. We next examined whether the number of infiltrated cells into the heart was also increased and, if so, what kinds of cells infiltrated into the heart. Immunohistochemical analysis using specific antibodies revealed that there was infiltration of granulocytes, macrophages, and T lymphocytes in the hearts of 4 days after MI. More granulocytes were observed in the hearts of the three treatment groups with G-CSF (pre-GS, 56.8 ± 15.0/10^{3}cells; post-GS, 62.2 ± 14.0/10^{3}cells; post-G, 58.7 ± 15.0/10^{3}cells) than in control group (32.1 ± 5.0/10^{3}cells, P<0.05) at 4 days after MI (Fig. 3*A*, *B*). There was no significant difference in the number of macrophages (Fig. 3*C*, *D*) and T lymphocytes (Fig. 3*E* and *F*) among the three treatment groups with G-CSF and control group.

Mobilization of BM cells

We next examined whether BM cells were infiltrated into the heart by using the mice whose BM was replaced by that of GFP-expressing mice. Because it was difficult to discriminate

GFP-expressing BM cells from other types of cells because of autofluorescence of MI hearts (Fig. 4*A*), we identified BM-derived cells by using anti-GFP antibody. Many GFP-positive cells were recognized in the border area of all the three treatment groups but not the control group (Fig. 4*B*). Most of GFP-positive cells were infiltrated blood cells (arrows in Fig. 4*B*), and some GFP-positive cells were observed at capillary walls (Fig. 4*C*). There were few GFP-positive cardiomyocytes (less than 0.01%) in the border area as well as in the infarcted area and the remote area. Therefore, we next compared the number of vessels in the border area. The number of capillaries in the border area after MI was much greater in all the three treatment groups (pre-GS, 8.0 ± 2.3/HPF; post-GS, 7.8 ± 1.7/HPF; post-G, 6.2 ± 1.9/HPF) than in the control group (2.0 ± 0.82/HPF, $P<0.05$; Fig. 4*D* and *E*).

Apoptotic cells in border area

We examined apoptotic cell death in the border area after MI. The number of TUNEL-positive cells in the border area of infarcted heart at Day 4 after MI was significantly smaller in the three treatment groups (pre-GS, 13.3 ± 3.2/10^3cells; post-GS, 10.8 ± 1.5/10^3cells; post-G, 12.8 ± 1.0/10^3cells, not significant among three groups) than in control group (30.7 ± 3.7/10^3cells, $P<0.05$; Fig. 4*F* and *G*). At Days 1 and 4, the number of TUNEL-positive cells was significantly smaller in Post-G group (Day 1, 73.8 ± 11.4/10^3cells; Day 4, 12.8 ± 1.0/10^3cells; Day 7, 4.7 ± 2.0/10^3cells) than in control group (Day 1, 116.0 ± 17.1/10^3cells; Day 4, 30.7 ± 3.7/10^3cells; Day 7, 4.2 ± 1.9/10^3cells, $P<0.05$; Fig. 5*A*). Furthermore, we examined double-immunohistochemical analysis to identify the cell type of apoptotic cells. We observed very few apoptotic cardiomyocytes at all the time points. The percentage of von Willebrand factor-positive cells in TUNEL-positive cells was significantly smaller in the Post-G group (Day 1, 0.8 ± 0.5%) than in control group (Day 1, 5.5 ± 1.5 %, $P<0.05$; Fig. 5*B*).

DISCUSSION

Because LV remodeling after MI determines subsequent cardiac function and prognosis, the inhibition of LV remodeling is clinically very important (1). After MI, many cardiomyocytes undergo cell death by the mechanisms of necrosis and apoptosis in the infarcted area, which is then replaced by fibrous tissue. The infarcted area is gradually extended by the subsequent death of cardiomyocytes and vascular cells in the border area and expanded by abnormal wall tension (2). Myocardial ischemia plays a critical role in the cardiomyocyte death in the border area after MI and thus greatly affects LV remodeling. It has been reported that a subset of BMSCs differentiates into cardiomyocytes when injected into peri-infarcted area, which results in regeneration of infarcted heart (3). Moreover, it has been reported that pretreatment with G-CSF and SCF attenuates LV remodeling after MI (4). Although these results suggest that the cytokine treatment is beneficial to prevent LV remodeling, the cytokine treatment was started before MI and thus this protocol cannot be applied to humans. Furthermore, the molecular mechanism of how the cytokine treatment repairs the infarcted heart is not fully understood. In the present study, 1) cytokine treatments started after MI were as effective as the pretreatment; 2) there was no significant difference in all parameters, including fibrotic area, cardiac function, and survival rate between the treatment with G-CSF alone and the combination treatment with G-CSF and SCF; 3) more capillaries were observed in the border area of the treatment groups with G-CSF compared with control group and SCF alone group, and the number of apoptotic cells was smaller in the three cytokine treatment groups with G-CSF than in control group.

It is very important to determine whether the combination therapy of G-CSF and SCF has additive effects on LV remodeling and cardiac function. Although it was reported that the combined treatment with G-CSF and SCF synergistically increased mobilization of BMSCs, it remains unknown whether the combined treatment also has synergistic effects on MI heart. Therefore, we compared the effects of G-CSF alone or SCF alone with those of combination treatment on LV remodeling and cardiac function after MI. Although the treatment with G-CSF alone showed effects similar to the combination treatment, the treatment with SCF alone could neither prevent LV remodeling nor improve survival rate after MI. It was previously reported that continuous treatment with SCF alone failed to induce any detectable change in the number of WBC throughout first 5 days and that a transient increase in WBC was increased at Day 7 after treatment in normal mice (16). Treatment with G-CSF alone increased the number of WBC at Day 4 after treatment. The different ability of BMSC mobilization between G-CSF and SCF may cause the different effects on LV remodeling after MI. These results suggest that G-CSF treatment started after MI is as beneficial as the pretreatment or the combination treatment with G-CSF and SCF to prevention of LV remodeling.

It has been reported that G-CSF induces the mobilization of BMSCs from BM into the peripheral blood circulation (17). There were more capillaries in the border area of all the cytokine treatment groups with G-CSF than in control group after MI, and a part of the cells constituting the capillary wall were derived from BM cells. There were few GFP-positive cardiomyocytes in the hearts in spite of the cytokine therapy. We think two possible mechanisms by which the cytokine therapy has beneficial effects on MI heart. One mechanism is that the cytokine therapy mobilizes BMSCs into MI heart and induces angiogenesis. Several lines of evidence suggest that BMSCs injected into myocardium induce angiogenesis (18, 19). Another mechanism is that the number of apoptotic endothelial cells is decreased by the cytokine therapy. The number of both von Willebrand factor and TUNEL-positive cells was significantly smaller in the Post-G group than in the control group. These mechanisms may result in an increase in capillary density leading to a decrease in apoptosis of cardiac myocytes in the border area. Recently, we observed that G-CSF induced activation of Akt, which has been reported to play an important role in cell survival and angiogenesis (20), in the border area after MI in swine (unpublished data). These results suggest that an increase in Akt activity by G-CSF may be also associated with an increase in the number of capillary vessels and a decrease in the number of apoptotic cells in the border area, resulting in better myocardial perfusion and less remodeling in the border area. Moreover, we recently examined whether G-CSF influences expression level of an angiogenic growth factor, vascular endothelial growth factor (VEGF; 21), after MI in swine. The expression of VEGF protein in the border area was increased in G-CSF-treated group than in the control group after MI (unpublished data). Further studies are needed to clarify what kinds of growth factors and cytokines are involved in angiogenic effects of the cytokine therapy in mouse MI model, and it also remains to be determined which cells (e.g., hematopoietic stem cells, mesenchymal stem cells, and endothelial progenitor cells) become vascular cells and whether neovascularization is a major mechanism for G-CSF-induced prevention of LV remodeling after MI.

ACKNOWLEDGMENTS

We thank to R. Kobayashi, E. Fujita, M. Watanabe, M. Iida, and A. Ohkubo for technical assistance. This work was supported by Takeda Medical Research Foundation, Uehara Memorial Foundation, Grant-in-Aid of The Japan Medical Association, The Kato Memorial Trust for Nambyo Research and Takeda Science Foundation.

REFERENCES

1. Pfeffer, M. A., and Braunwald, E. (1990) Ventricular remodeling after myocardial infarction. Experimental observations and clinical implications. *Circulation* **81,** 1161–1172

2. Krijnen, P. A., Nijmeijer, R., Meijer, C. J., Visser, C. A., Hack, C. E., and Niessen, H. W. (2002) Apoptosis in myocardial ischaemia and infarction. *J. Clin. Pathol.* **55,** 801–811

3. Orlic, D., Kajstura, J., Chimenti, S., Jakoniuk, I., Anderson, S. M., Li, B., Pickel, J., McKay, R., Nadal-Ginard, B., Bodine, D. M., et al. (2001) Bone marrow cells regenerate infarcted myocardium. *Nature* **410,** 701–705

4. Orlic, D., Kajstura, J., Chimenti, S., Limana, F., Jakoniuk, I., Quaini, F., Nadal-Ginard, B., Bodine, D. M., Leri, A., and Anversa, P. (2001) Mobilized bone marrow cells repair the infarcted heart, improving function and survival. *Proc. Natl. Acad. Sci. USA* **98,** 10344–10349

5. Davani, S., Marandin, A., Mersin, N., Royer, B., Kantelip, B., Herve, P., Etievent, J. P., and Kantelip, J. P. (2003) Mesenchymal progenitor cells differentiate into an endothelial phenotype, enhance vascular density, and improve heart function in a rat cellular cardiomyoplasty model. *Circulation* **108,** 253–258

6. Mangi, A. A., Noiseux, N., Kong, D., He, H., Rezvani, M., Ingwall, J. S., and Dzau, V. (2003) Mesenchymal stem cells modified with Akt prevent remodeling and restore performance of infarcted hearts. *Nat. Med.* **9,** 1195–1201

7. Harada, K., Sugaya, T., Murakami, K., Yazaki, Y., and Komuro, I. (1999) Angiotensin II type 1A receptor knockout mice display less left ventricular remodeling and improved survival after myocardial infarction. *Circulation* **100,** 2093–2099

8. Takimoto, E., Yao, A., Toko, H., Takano, H., Shimoyama, M., Sonoda, M., Wakimoto, K., Takahashi, T., Akazawa, H., Mizukami, M., et al. (2002) Sodium calcium exchanger plays a key role in alteration of cardiac function in response to pressure overload. *FASEB J.* **16,** 373–378

9. Li, Y., Takemura, G., Kosai, K., Yuge, K., Nagano, S., Esaki, M., Goto, K., Takahashi, T., Hayakawa, K., Koda, M., et al. (2003) Postinfarction Treatment With an Adenoviral Vector Expressing Hepatocyte Growth Factor Relieves Chronic Left Ventricular Remodeling and Dysfunction in Mice. *Circulation* **107,** 2499–2506

10. Toko, H., Zhu, W., Takimoto, E., Shiojima, I., Hiroi, Y., Zou, Y., Oka, T., Akazawa, H., Mizukami, M., Sakamoto, M., et al. (2002) Csx/Nkx2-5 is required for homeostasis and survival of cardiac myocytes in the adult heart. *J. Biol. Chem.* **277,** 24735–24743

11. Hadjantonakis, A. K., and Nagy, A. (2001) The color of mice: in the light of GFP-variant reporters. *Histochem. Cell Biol.* **115,** 49–58

12. Yoder, M. C., Hiatt, K., Dutt, P., Mukherjee, P., Bodine, D. M., and Orlic, D. (1997) Characterization of definitive lymphohematopoietic stem cells in the day 9 murine yolk sac. *Immunity* **7,** 335–344

13. Krause, D. S., Ito, T., Fackler, M. J., Smith, O. M., Collector, M. I., Sharkis, S. J., and May, W. S. (1994) Characterization of murine CD34, a marker for hematopoietic progenitor and stem cells. *Blood* **84,** 691–701

14. To, L. B., Haylock, D. N., Simmons, P. J., and Juttner, C. A. (1997) The biology and clinical uses of blood stem cells. *Blood* **89,** 2233–2258

15. Clark, S. C., and Kamen, R. (1987) The human hematopoietic colony-stimulating factors. *Science* **236,** 1229–1237

16. Molineux, G., Migdalska, A., Szmitkowski, M., Zsebo, K., and Dexter, T. M. (1991) The effects on hematopoiesis of recombinant stem cell factor (ligand for c-kit) administered in vivo to mice either alone or in combination with granulocyte colony-stimulating factor. *Blood* **78,** 961–966

17. Tanaka, J., Miyake, T., Shimizu, T., Wakayana, T., Tsumori, M., Koshimura, K., Murakami, Y., and Kato, Y. (2002) Effect of continuous subcutaneous administration of a low dose of G-CSF on stem cell mobilization in healthy donors: a feasibility study. *Int. J. Hematol.* **75,** 489–492

18. Kamihata, H., Matsubara, H., Nishiue, T., Fujiyama, S., Tsutsumi, Y., Ozono, R., Masaki, H., Mori, Y., Iba, O., Tateishi, E., et al. (2001) Implantation of Bone Marrow Mononuclear Cells Into Ischemic Myocardium Enhances Collateral Perfusion and Regional Function via Side Supply of Angioblasts, Angiogenic Ligands, and Cytokines. *Circulation* **104,** 1046–1052

19. Strauer, B. E., Brehm, M., Zeus, T., Köstering, M., Hernandez, A., Sorg, V. R., Kögler, G., and Wernet, P. (2002) Repair of infarcted myocardium by autologous intracoronary mononuclear bone marrow cell transplantation in humans. *Circulation.* **106,** 1913–1918

20. Koc, O. N., and Gerson, S. L. (2003) Akt helps stem cells heal the heart. *Nat. Med.* **9,** 1109–1110

21. Kupatt, C., Hinkel, R., Vachenauer, R., Horstkotte, J., Raake, P., Sandner, T., Kreuzpointner, R., Muller, F., Dimmeler, S., Feron, O., et al. (2003) VEGF165 transfection decreases postischemic NF-kappa B-dependent myocardial reperfusion injury in vivo: role of eNOS phosphorylation. *FASEB J.* **17,** 705–707

Received August 19, 2003; accepted January 20, 2004.

Table 1

Hemodynamic parameter after MI

	Sham (n=5)	Control (n=5)	Pre-GS (n=10)	Post-GS (n=16)	Post-G (n=14)	Post-S (n=9)
LVP (mmHg)	103.1±13.9	61.8±11.7	87.3±16.1*	89.9±17.5*	85.7±6.7*	63.3±5.5
LVEDP (mmHg)	2.0±0.8	13.3±6.8	4.1±2.5*	3.3±3.3*	4.2±2.6*	12.4±2.5
dP/dt (mmHg/s)	6034±302	2048±558	2860±567*	3241±710*	2558±373*	2106±466
–dP/dt (mmHg/s)	5805±364	2018±459	2778±567*	3169±703*	2598±371*	2011±479

LVP, left ventricular systolic pressure; LVEDP, left ventricular end-diastolic pressure; dP/dt and –dP/dt, positive and negative first derivatives for maximal rates of left ventricular pressure development.
Values are mean ± SD. *$P < 0.05$ vs. Control group.

Fig. 1

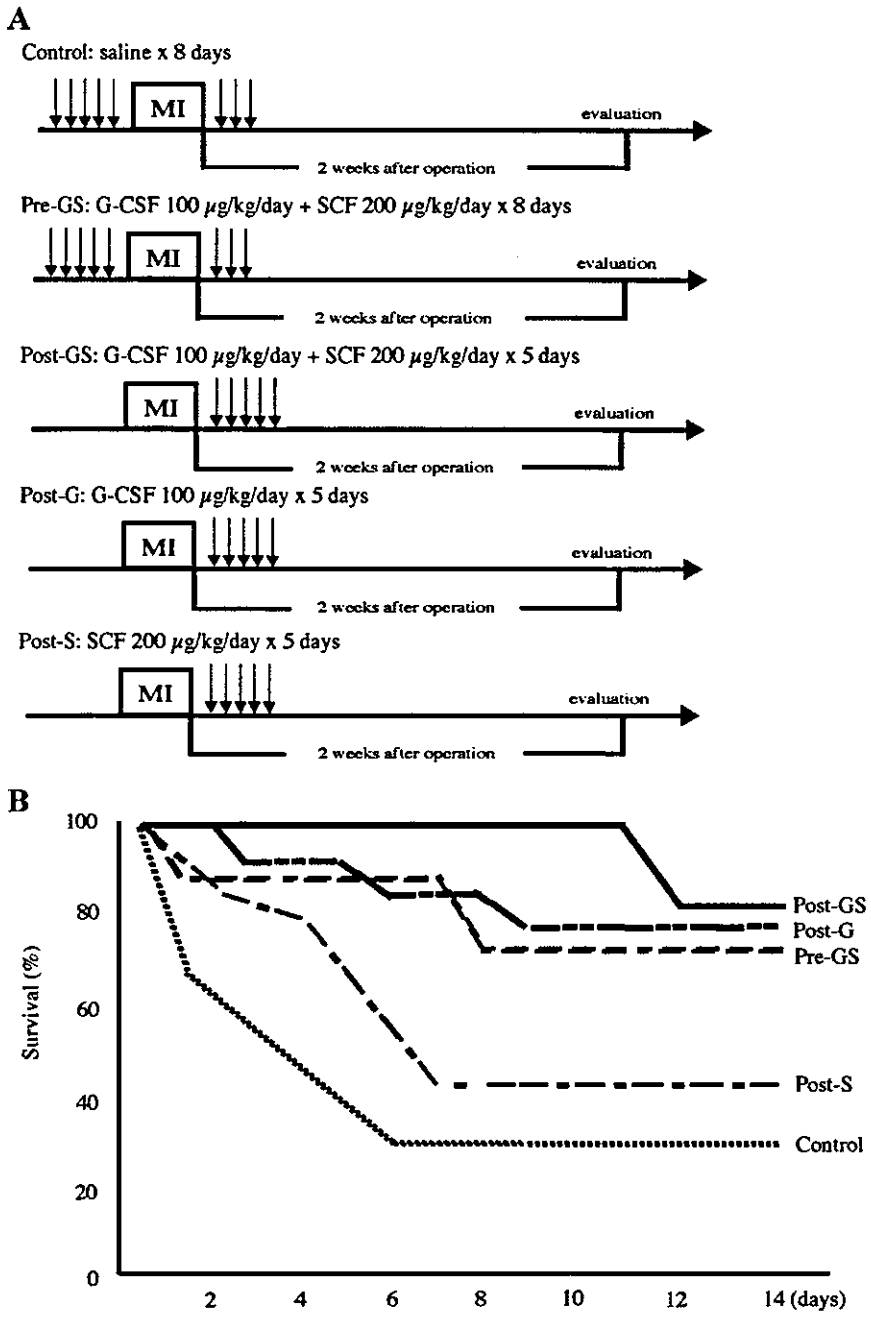

Figure 1. Protocol of the cytokine treatment and survival rate. *A)* Mice in pretreatment group (Pre-GS) were injected subcutaneously (s.c.) with SCF (200 μg/kg/day) and G-CSF (100 μg/kg/day) from 5 days before MI until 3 days after MI (n=16). Mice in post-treatment groups were injected s.c. with G-CSF alone (Post-G; n=20), SCF alone (Post-S; n=21), or SCF and G-CSF once a day for 5 days after MI (Post-GS; n=20). Mice in control group (Control) were injected with saline for 8 days before and after MI (n=22). *B)* Survival rates of mice at 14 days were higher in 3 treatment groups with G-CSF than in control group in Kaplan-Meier method.

Fig. 2

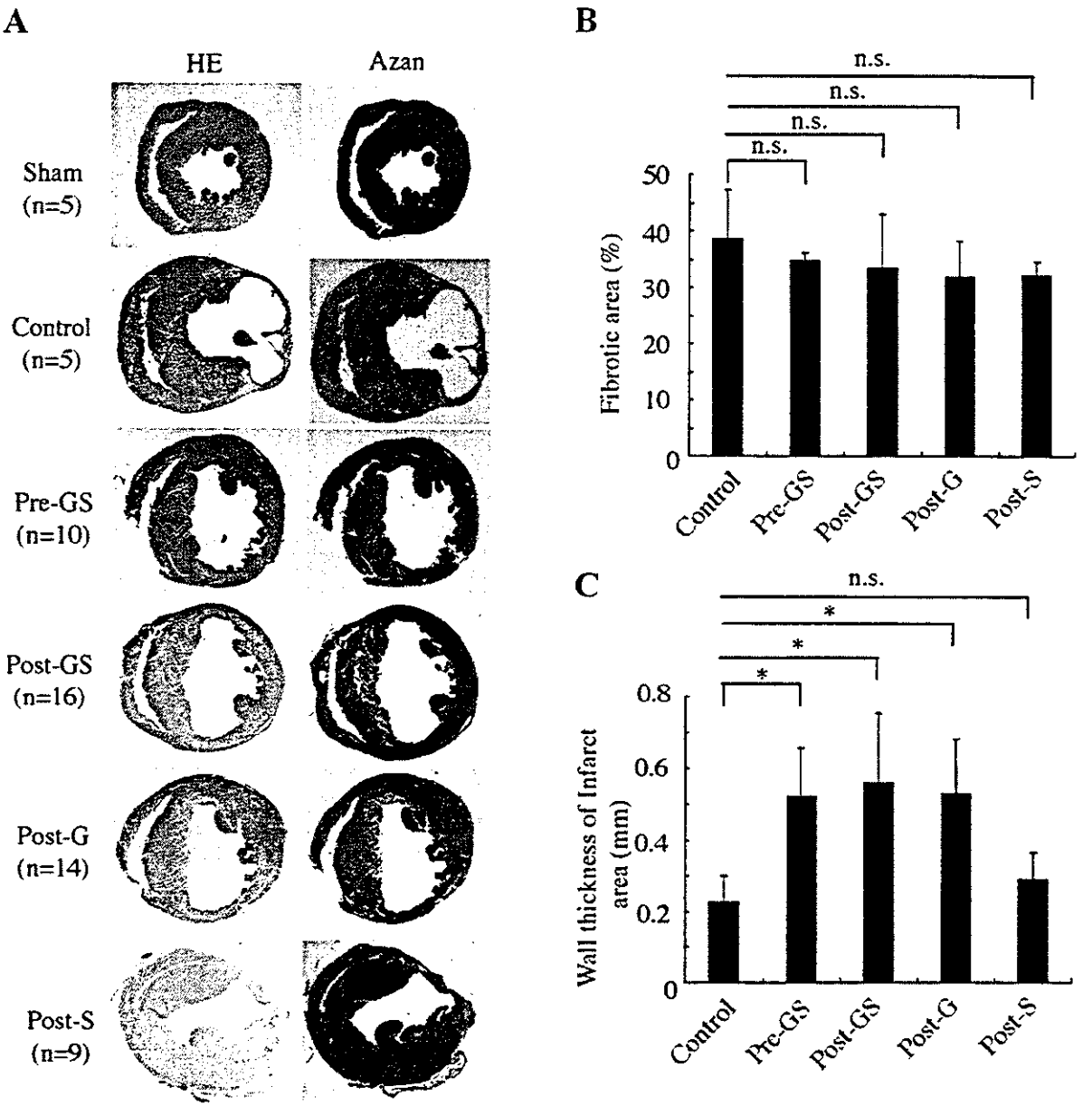

Figure 2. Morphological analysis. We examined hemodynamic parameters of the survived mice (Sham, n=5; Control, n=5; Pre-GS, n=10; Post-GS, n=16; Post-G, n=14; Post-S, n=9) at 2 weeks after MI by cardiac catheterization and subsequently performed histological analysis. ***A***) Light microscopic analysis in hematoxylin-eosin (HE) staining and Azan-Mallory staining. LV free wall was thinner in heart of control group and Post-S group than in heart of Post-G, Post-GS, and Pre-GS groups (HE: left panel). Infarct area was replaced completely by fibrotic tissue in control group, while remained myocardium was observed in the hearts of all the treatment groups with G-CSF (Azan: right panel). ***B***) Fibrotic area in the whole LV area. There was no significant difference in the percentages of fibrotic area among the treatment groups and control group (n.s., not significant.). ***C***) Wall thickness of infarct area was thinner in hearts of control group and Post-S group than in hearts of Post-G, Post-GS, and Pre-GS groups (*P<0.05).

Fig. 3

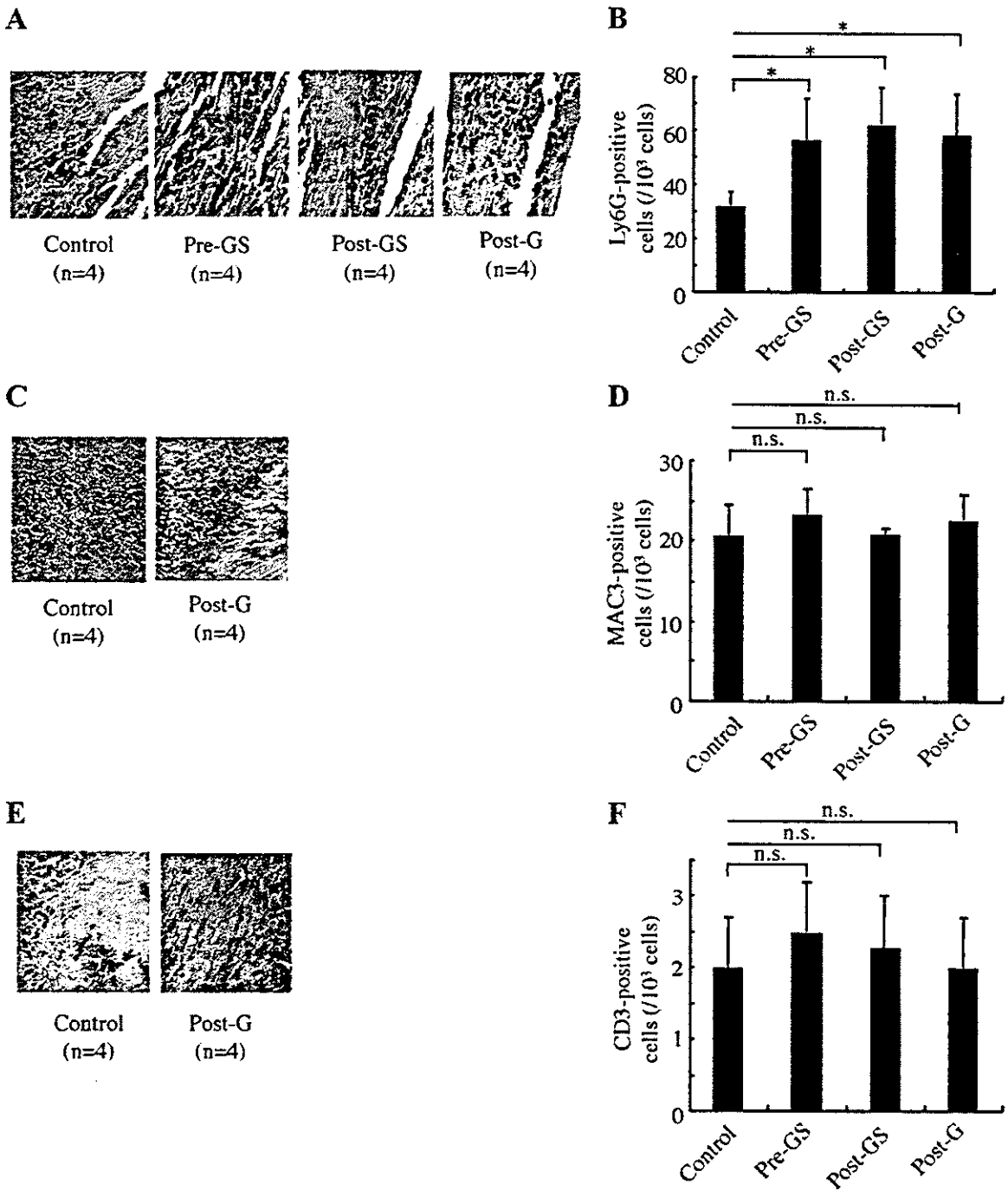

Figure 3. Inflammatory cells in the heart. ***A***, ***B***) The number of Ly6G-positive cells (granulocytes) at the border area of infarcted heart was greater in the three treatment groups than in control group (*$P<0.05$) at 4 days after MI. There was no significant difference in the number of MAC3-positive cells (macrophages; ***C***, ***D***) and CD3-positive cells (T-lymphocytes; ***E***, ***F***) among the three treatment groups and control group.

Fig. 4

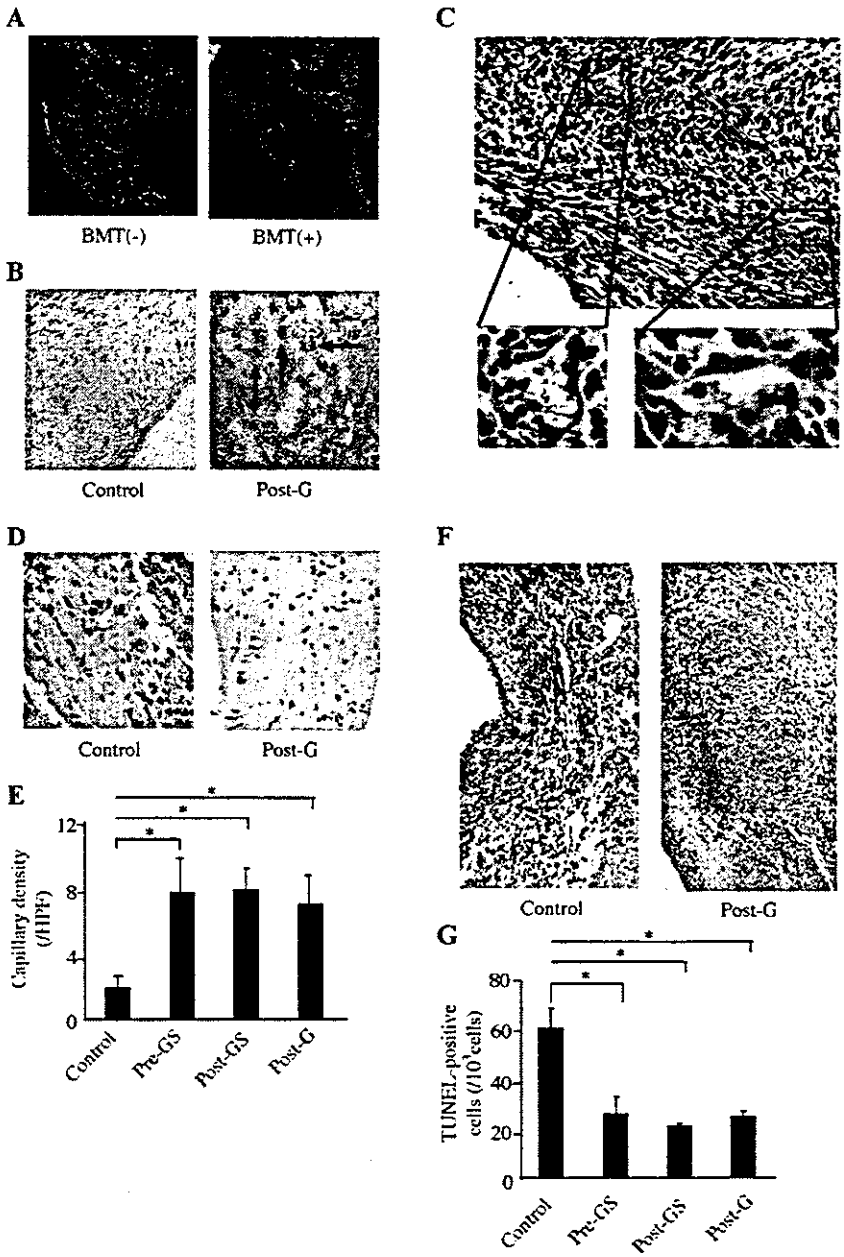

Figure 4. GFP-positive cells, capillary density and TUNEL-positive cells after MI. *A)* Non-specific autofluorescence was recognized at the infarcted and border areas. BMT (–), infarcted heart of the mice without BM transplantation; BMT (+), infarcted heart of the mice whose BM was replaced with that of GFP mice. *B)* Many GFP-positive cells (brown), which were mainly infiltrated blood cells, were recognized at the border area after MI in the three treatment groups with G-CSF. *C)* GFP-positive cells were observed at capillary wall after MI in all the treatment groups. *D)* The capillary density was examined by measuring PECAM-1-positive cells. *E)* The density of capillaries at the border area was more increased in all the cytokine groups than in control group (**P*<0.05). There was no significant difference of the capillary densities among the three treatment groups with G-CSF. *F)* Apoptotic cells at Day 4 after MI. *G)* The number of TUNEL-positive cells at the border area was less in all the treatment groups than in control group (**P*<0.05). There was no significant difference in the number of TUNEL-positive cells among the three treatment groups.

Fig. 5

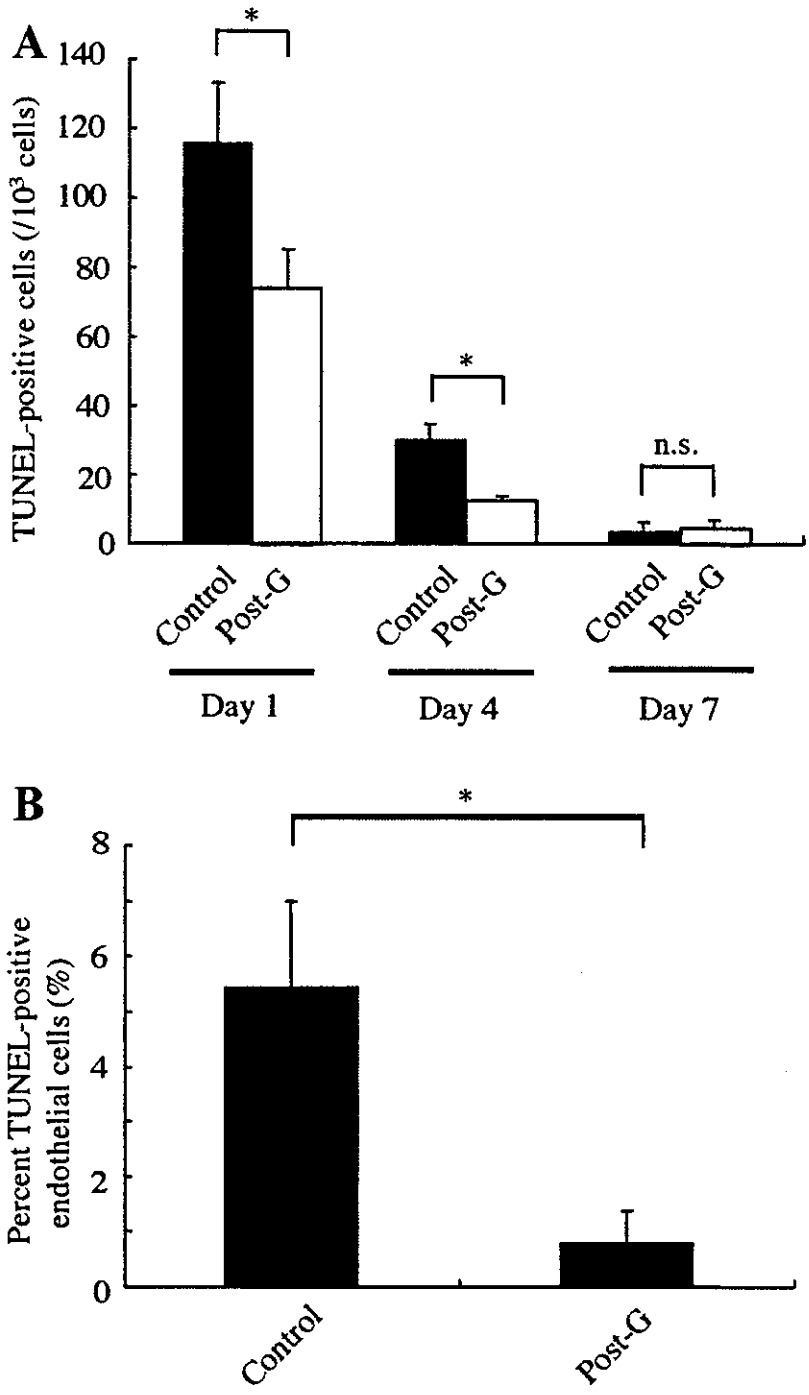

Figure 5. Apoptotic endothelial cell and non-endothelial cell death. ***A)*** At Day 1 and Day 4, the number of TUNEL-positive cells was significantly smallerin the Post-G group than in control group (**P*<0.05). ***B)*** We checked double-immunohistochemical analysis to identify for the apoptotic endothelial cells at Day 1 after MI. The percentage of von Willebrand factor-positive cells in TUNEL-positive cells was significantly smaller in the Post-G group (**P*<0.05).

Angiotensin II Type 1a Receptor Is Involved in Cell Infiltration, Cytokine Production, and Neovascularization in Infarcted Myocardium

Haruhiro Toko, Yunzeng Zou, Tohru Minamino, Masaya Sakamoto, Masanori Sano, Mutsuo Harada, Toshio Nagai, Takeshi Sugaya, Fumio Terasaki, Yasushi Kitaura, Issei Komuro

Objective—Angiotensin II is critically involved in left ventricular remodeling after myocardial infarction. Neovascularization has been thought to prevent the development of left ventricular remodeling and deterioration to heart failure. To elucidate the role of angiotensin II in neovascularization during cardiac remodeling, we induced myocardial infarction in angiotensin II type1a receptor (AT1) knockout (KO) mice.

Methods and Results—There were more vessels in the border zone of infarcted hearts of wild-type (WT) mice and AT1KO mice at 14 days after operation, compared with in the left ventricle of sham-operated mice, and the number was larger in WT mice than in AT1KO mice. Consistent with these observations, the infarcted heart of AT1KO mice expressed lower levels of matrix metalloproteinase and endothelial nitric oxide synthase activity. More inflammatory cells such as granulocytes and macrophages were infiltrated in the infarcted hearts of WT mice than AT1KO mice at 4 days. A variety of cytokines and chemokines were increased in infarcted hearts of WT and AT1KO mice, and many of them were more remarkable in WT mice than in AT1KO mice at 14 days.

Conclusions—AT1 plays a critical role in inflammatory cell infiltration, cytokine production, and neovascularization in infarcted hearts. (***Arterioscler Thromb Vasc Biol.* 2004;24:664-670.**)

Key Words: angiotensin II ■ AT1 receptor ■ neovascularization ■ myocardial infarction ■ cardiac remodeling

Left ventricular remodeling after myocardial infarction (MI) causes progression of heart failure and death. The remodeling process is characterized by progressive expansion of the initial infarct area and dilation of the left ventricular lumen, with cardiomyocyte replacement by fibrous tissue deposition in the ventricular wall. Once these processes develop, the infarcted heart accelerates the deterioration of ventricular dysfunction, leading to heart failure.

See page 622

Accumulating evidence has suggested that the renin-angiotensin system (RAS) plays an important role in left ventricular remodeling after MI, and that inhibition of RAS with angiotensin-converting enzyme (ACE) inhibitors and angiotensin II (AngII) type 1a receptor (AT1) blockers suppresses the cardiac remodeling and reduces the mortality after MI in clinical studies and experimental models.[1–3] We also reported that AngII plays a critical role in cardiac remodeling and mortality after MI using AT1 knockout (KO) mice.[4] Although cardiac dysfunction was more prominent and mortality was higher in wild-type (WT) mice than AT1KO mice after MI,[4] the precise mechanism of how AngII induces left ventricular remodeling remains unknown.

It has been reported that neovascularization within the infarcted tissue is an integral component of the remodeling process and that induction of neovascularization reduces infracted area and mortality.[5] There are several controversial reports regarding the effects of AngII on vascularization. Some reports have shown that AngII induces neovascularization in tumors, ischemic legs, and retina,[6–8] but others have reported that inhibition of RAS stimulates neovascularization.[9] It has also been reported that an ACE inhibitor does not inhibit vascular growth during the early phase of post-infarcted cardiac remodeling and scar formation.[10] To elucidate the role of AngII in neovascularization in the heart, we induced MI and examined the number of vessels in AT1KO mice.

Methods

Animals

Eight-week-old male WT mice and AT1KO mice[11] from the same genetic background were used in the present study (SLC, Shizuoka,

Received December 22, 2003; revision accepted January 21, 2004.

From the Department of Cardiovascular Science and Medicine (H.T., Y.Z., T.M., M. Sakamoto, M. Sano, M.H., T.N., I.K.), Chiba University Graduate School of Medicine, Chiba, Japan; Discovery Laboratory (T.S.), Tanabe Seiyaku Co, Ltd, Osaka, Japan; and Third Department of Internal Medicine (F.T., Y.K.), Osaka Medical College, Osaka, Japan.

Correspondence to Dr Issei Komuro, Department of Cardiovascular Science and Medicine, Chiba University Graduate School of Medicine, 1-8-1 Inohana, Chuo-ku, Chiba 260-8670, Japan. E-mail komuro-tky@umin.ac.jp

Arterioscler Thromb Vasc Biol. is available at http://www.atvbaha.org DOI: 10.1161/01.ATV.0000122361.63827.ab